Blocking Vascular Endothelial Growth Factor-A Inhibits the Growth of Pituitary Adenomas and Lowers Serum Prolactin Level in a Mouse Model of Multiple Endocrine Neoplasia Type 1

Nina Korsisaari, Jed Ross, Xiumin Wu, Marcin Kowanetz, Navneet Pal, Linda Hall, Jeffrey Eastham-Anderson, William F. Forrest, Nicholas Van Bruggen, Franklin V. Peale, and Napoleone Ferrara

Abstract

Purpose: Multiple endocrine neoplasia type 1 (MEN1) is defined clinically by the combined occurrence of multiple tumors, typically of the parathyroid glands, pancreatic islet cells, and anterior pituitary gland. A mouse model with a heterozygous deletion of the *Men1* gene recapitulates the tumorigenesis of MEN1. We wished to determine the role of vascular endothelial growth factor (VEGF)-A in the vascularization and growth of MEN1-associated tumors, with an emphasis on pituitary adenomas.

Experimental Design: To investigate whether tumor growth in *Men1*$^{+/-}$ mice is mediated by VEGF-A dependent angiogenesis, we carried out a monotherapy with the anti–VEGF-A monoclonal antibody (mAb) G6-31. We evaluated tumor growth by magnetic resonance imaging and assessed vascular density in tissue sections. We also measured hormone levels in the serum.

Results: During the treatment with mAb G6-31, a significant inhibition of the pituitary adenoma growth was observed, leading to an increased mean tumor doubling-free survival compared with mice treated with a control antibody. Similarly, the growth of s.c. pituitary adenoma transplants was effectively inhibited by administration of anti–VEGF-A mAb. Serum prolactin was lowered by mAb G6-31 treatment but not by control antibody, potentially providing a new therapeutic approach for treating the hormonal excess in MEN1 patients. Additionally, the vascular density in pancreatic islet tumors was significantly reduced by the treatment.

Conclusions: These results suggest that VEGF-A blockade may represent a nonsurgical treatment for benign tumors of the endocrine system.

Angiogenesis, the formation of a refined vascular network by endothelial cell sprouting from preexisting vessels, is essential for embryonic development and for the growth of normal adult tissues (1, 2). Angiogenesis is also required for wound healing and reproductive function. It is now well established that angiogenesis also plays an important role in the pathogenesis of several disorders (3, 4). Endocrine glands are highly vascularized organs, reflecting the need to rapidly deliver hormones in the bloodstream and respond to regulatory feedbacks, and several angiogenic factors have been described in normal and neoplastic glands (reviewed in ref. 5). These include members of the vascular endothelial growth factor (VEGF) and fibroblast growth factor families (5) and the recently described EG-VEGF (6–8). One of the best characterized positive regulators of angiogenesis is VEGF-A (9). In mammals, VEGF-A belongs to a gene family also including VEGF-B, VEGF-C, VEGF-D, and PlGF (10). VEGF-A primarily binds to two high-affinity receptor tyrosine kinases, VEGF receptor (VEGFR)-1 (Flt-1) and VEGFR-2 (Flk-1/KDR), the latter being the major transmitter of vascular endothelial cell mitogenic signals of VEGF-A (11, 12).

Multiple endocrine neoplasia (MEN) is a disorder characterized by the incidence of tumors involving two or more endocrine glands (13). A patient is classified with MEN type 1 (MEN1) when a combined occurrence of tumors in the parathyroid glands, the pancreatic islet cells, and the anterior pituitary is identified (14). Mutations in *MEN1* gene were discovered to underlie the disorder (15), which commonly result in a truncation or absence of the protein menin (reviewed in ref. 16). With the added finding of a frequent loss of the remaining allele in the tumors (17–19), *MEN1* has been classified as a tumor suppressor gene. Whereas MEN1 is largely inherited as an autosomal dominant disorder, *de novo* mutations of *MEN1* gene have been identified as the cause of sporadic cases of MEN1.

The function of menin remains unclear. The ubiquitously expressed, predominantly nuclear 610-amino-acid protein has been suggested to be involved in transcriptional regulation, DNA processing and repair, and cytoskeletal organization

Authors' Affiliation: Genentech, Inc., South San Francisco, California
Received 6/26/07; revised 9/16/07; accepted 9/27/07.
The costs of publication of this article were defrayed in part by the payment of page charges. This article must therefore be hereby marked *advertisement* in accordance with 18 U.S.C. Section 1734 solely to indicate this fact.
Note: Supplementary data for this article are available at Clinical Cancer Research Online (http://clincancerres.aacrjournals.org/).
N. Korsisaari and J. Ross contributed equally to this work.
Requests for reprints: Napoleone Ferrara, Genentech, Inc., 1DNA Way, South San Francisco, CA 94080. Phone: 650-225-2968; Fax: 650-225-4265; E-mail: nf@gene.com.

doi:10.1158/1078-0432.CCR-07-1552

through its *in vitro* interactions with proteins that are part of the pathways mentioned above (reviewed in ref. 20). None of the protein interactions identified thus far, however, provide an explanation to the tumorigenicity in MEN1.

Current standard of treatment for neuroendocrine pancreatic tumors (in some clinical series, >50% are gastrinomas and 10-30% are insulinomas) is reduction of basal acid output in the case of gastrinomas, whereas surgery is seen as the optimal treatment for insulinomas. The treatment for pituitary tumors consists of selective surgery with varying medical therapy depending on the hormonal profile, whereas the definitive treatment for parathyroid tumors is a surgical removal of the overactive gland. However, there is variability to the degree and timing of the parathyroidectomy (21). The latest developments on the generation of new approaches to the diagnosis and treatment of MEN1 have recently been reviewed elsewhere (22).

Through homologous recombination, exons 3 to 8 of the mouse gene *Men1* have been targeted for deletion (23). By 9 months of age, heterozygous *Men1* mice were reported to develop pancreatic islet lesions with additional frequent observations of parathyroid adenomas. Larger, more numerous tumors in pancreatic islets, parathyroids, thyroid, adrenal cortex, and pituitary were seen by 16 months of age (23), features remarkably similar to the human disorder.

Ample evidence exists indicating that blocking VEGF-A–mediated angiogenesis results in tumor suppression (24–28), and anti–VEGF-A approaches have been used in treatment of various preclinical models of human malignant cancer cell lines. Tumor xenografts, however, poorly recapitulate tumor development in a natural setting. Furthermore, there are as yet few examples of successful long-term use of anti-VEGF mAbs in preclinical models of benign tumors (29).

To investigate the role of VEGF-A in the development of endocrine tissue–specific adenomas, we took advantage of recently described cross-reactive neutralizing anti–VEGF-A monoclonal antibodies (mAb; ref. 30). We tested the effects of VEGF-A neutralization in a naturally occurring nonmalignant tumor model, the *Men1*$^{+/-}$ mouse model of MEN1. Tumor volume of pituitary adenomas in *Men1*$^{+/-}$ mice as well as s.c. pituitary tumor transplants in BALB/c nude mice was analyzed after treatment with anti–VEGF-A mAb. Finally, we asked whether treatment with anti–VEGF-A mAb could lower the elevated hormone levels associated with MEN1.

Materials and Methods

Animal husbandry. *Men1*$^{+/-}$ mice (23) were obtained from The Jackson Laboratory and BALB/c nude mice from Charles River Laboratories, Inc. Experimental *Men1*$^{+/-}$ female mice of mixed 129-FVB background were obtained by intercrossing *Men1*$^{+/-}$ males and females. Mice were housed in microisolator cages in a barrier facility and fed *ad libitum*. Maintenance of animals and experimental protocols were conducted following federal regulations and approved by Institutional Animal Care and Use Committee.

Grafting of pituitary tumors to dorsal flank. S.c. pituitary adenoma transplants were established in 6- to 8-week-old female BALB/c nude mice according to the following procedure. A single *in situ* pituitary adenoma from a *Men1*$^{+/-}$ mouse was extracted and minced into ~1-mm^3 pieces, mixed with BD Matrigel Matrix Basement Membrane, and inoculated s.c. in 200-μL volume to the dorsal flank of BALB/c nude mice. Four months later, a single s.c. tumor (approximate volume, 900 mm^3) was extracted, minced, mixed with Matrigel, and inoculated as described above to establish a cohort of mice with pituitary adenoma transplants.

Treatment of mice with mAb G6-31 and control IgG antibodies. The cross-reactive anti–VEGF-A mAb G6-31 was derived from human Fab phage libraries (30). To generate a mAb suitable for long-term administration in immunocompetent mice, the variable domains were grafted into murine IgG2a constant domain. I.p. injection at 5 mg/kg of mAb G6-31 or isotype-matched control IgG (anti-GP120) was given once a week in a 100- to 200-μL volume in PBS. Treatment of *Men1*$^{+/-}$ mice harboring pituitary adenomas *in situ* with mAb G6-31 (n = 8) or control IgG (n = 9) was started at 13.5 to 14.5 months of age and continued for 67 days or until mice were found moribund. BALB/c nude mice with a s.c. pituitary adenoma transplant were treated with control IgG (n = 23) or mAb G6-31 (n = 35), starting 4 months after grafting. The treatment continued for 35 days or until mice were found moribund or tumor volume had reached 3,000 mm^3.

Magnetic resonance imaging of primary pituitary tumors. Magnetic resonance images were acquired on a 9.4T horizontal bore magnet (Oxford Instruments Ltd.) and controlled by a Varian Inova console (Varian, Inc.) using a 3-cm volume coil for transmission and reception (Varian). A fast spin echo imaging sequence was used with a repetition time of 4 s, echo train length of 8, echo spacing of 12 ms, effective echo time of 48 ms, and six averages. The image matrix was 128^2, with a field of view of $(20\ mm)^2$ and slice thickness of 0.5 mm. Mice were restrained in the prone position with 2% isoflurane in medical air, whereas body temperature was monitored with a rectal probe and maintained at 37°C with warm air for the duration of the 15-min image acquisition. After imaging, animals were allowed to recover on a heated surface followed by returning them to the housing facility.

Analysis of tumor volumes. Primary pituitary tumor volumes were calculated from magnetic resonance imaging data using three-dimensional regions of interest drawn in Analyze software (AnalyzeDirect, Inc.).

Tumor size of s.c. pituitary adenoma transplants was estimated with a caliper tool (Fred V. Fowler Co., Inc.) by measuring the largest tumor diameter and the diameter perpendicular to that. Tumor volume was calculated using the following formula: $V = \pi ab^2/6$, where a is the largest tumor diameter and b is the perpendicular diameter.

RNA sample preparation and quantitative PCR analysis. Total DNA-free RNA was prepared from flash-frozen pituitary adenomas or normal pituitary glands with RNeasy kit (Qiagen) according to the manufacturer's protocol. One-step quantitative reverse transcription-PCR was done in a total volume of 50 μL with SuperScript III Platinum One-Step qRT-PCR Kit (Invitrogen), 100 ng of total RNA, 45 nmol/L of each PCR primer, and 12.5 nmol/L TaqMan probe. To detect expression of the genes of interest, the following TaqMan Gene Expression Assay primers and probe mixes (Applied Biosystems) were used: *VEGF-A* (assay ID: Mm00437304_m1), *VEGFR-1* (assay ID: Mm00438980_m1), *VEGFR-2* (assay ID: Mm00440099_m1), *CD31* (assay ID: Mm00476702_m1), and *Tie-2* (assay ID: Mm01256900_m1). *GAPDH* expression was detected using primers and TaqMan probe synthesized in in-house facility (forward primer, ATGTTCCAGTATGACTCCACTCACG; reverse primer, GAAGACACCAGTAGACTCCACGACA; TaqMan probe, AAGCCCATCACCATCTTCCAGGAGCGAGA).

Reactions were carried out using Applied Biosystems 7500 Real-time PCR System with the following conditions: a reverse transcription step (15 min at 48°C) followed by denaturation step (2 min 95°C) and 40 cycles of 15 s at 95°C and 1 min at 60°C. Levels of gene expression in each sample were determined with the relative quantification method using *GAPDH* mRNA as an endogenous control.

Histologic analysis. Formalin-fixed tissue was dehydrated and embedded in paraffin, sectioned, and stained with H&E for histologic analysis following standard protocols.

Immunohistochemistry. Formalin-fixed, paraffin-embedded tissue sections were deparaffinized before quenching of endogenous peroxidase activity and blocking of endogenous biotin (Vector). Sections

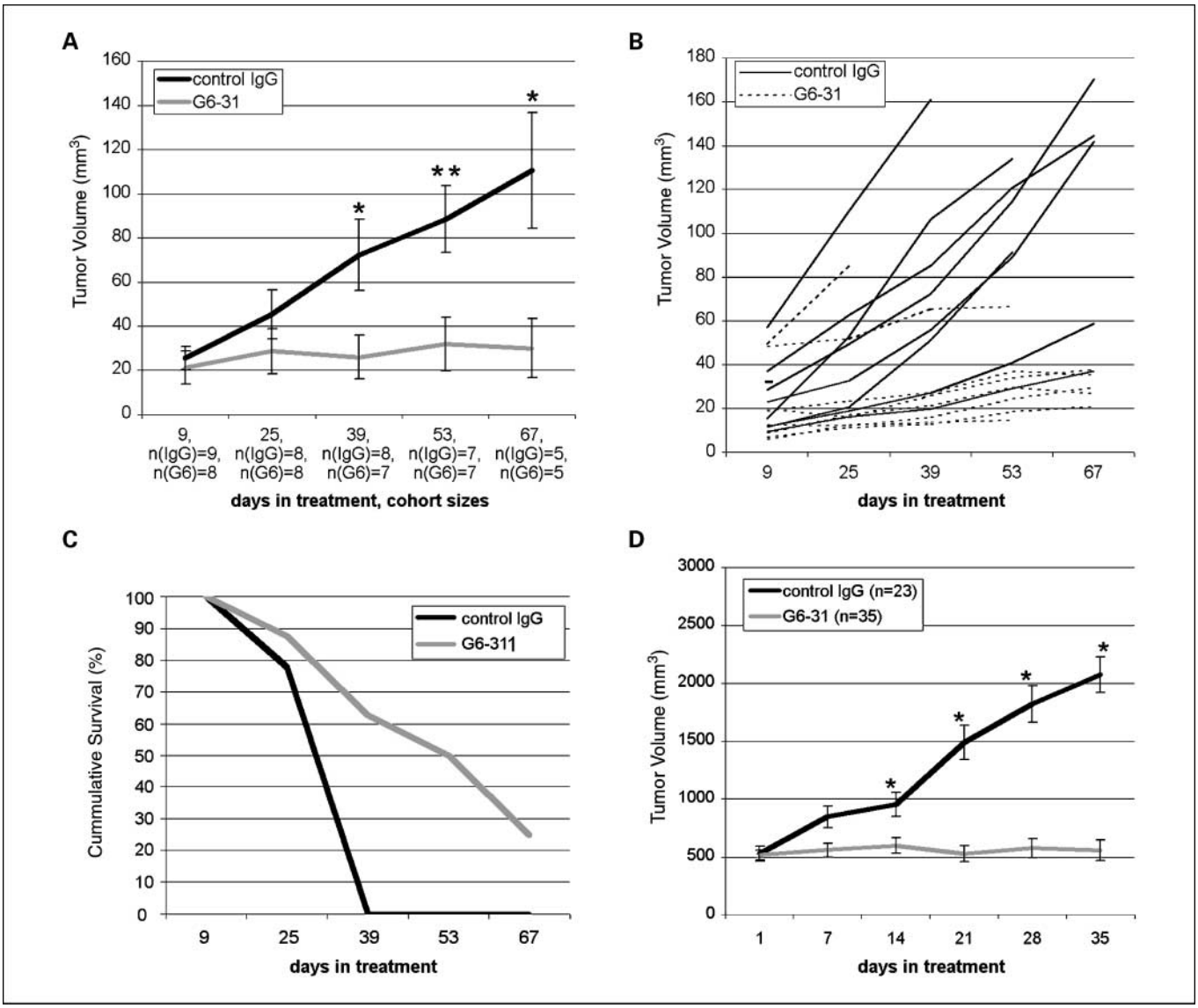

Fig. 1. Anti – VEGF-A treatment inhibits pituitary tumor growth. *A,* points, mean tumor volume of mice treated with control IgG (*black line*) or mAb G6-31 (*gray line*) at days 9, 25, 39, 53, and 67 of treatment; bars, SE. *n*, number of mice in the group. *B,* tumor volumes of individual mice treated with control IgG (*solid lines*) or mAb G6-31 (*broken lines*). Seven mice were euthanized before the end point of the study (lines ending before 67-d time point). *C,* tumor doubling free-survival of mice treated with control IgG (*black line*) or mAb G6-31 (*gray line*) assessed at days 9, 25, 39, 53, and 67 after treatment onset. Mouse number per time point and treatment group was 7 to 9 for days 9 to 53, and 5 for day 67. *, $P < 0.03$; **, $P < 0.005$. *D,* points, mean tumor volume of s.c. pituitary tumor transplants from mice treated with control IgG (*black line*) or mAb G6-31 (*gray line*) at days 1, 7, 14, 21, 28, and 35 of treatment; bars, SE.

were further blocked for 30 min with 10% normal rabbit serum in PBS with 3% bovine serum albumin. Tissue sections were then incubated with primary antibodies for 60 min, with biotinylated secondary antibodies for 30 min, and with avidin-biotin complex reagent (Vector) for 30 min, followed by a 5-min incubation in Metal Enhanced DAB (Pierce). Sections were then counterstained with Mayer's hematoxylin. Primary antibodies used were goat anti-mouse prolactin at 0.10 μg/mL (R&D Systems) and rat anti-mouse pan-endothelial cell antigen, clone MECA-32, at 2 μg/mL (BD Biosciences). Secondary antibodies used were biotinylated rabbit anti-goat at 7.5 μg/mL (Vector) and biotinylated rabbit anti-rat at 2.5 μg/mL (Vector). MECA-32 staining required pretreatment with Target Retrieval (DAKO) at 99°C for 20 min. All other steps were done at room temperature.

For detection of mouse growth hormone, paraffin sections were treated as above except as noted: avidin-biotin and normal rabbit serum blocking steps were omitted; primary antibody, a rabbit polyclonal (Chemicon), was applied at a 1:2,000 dilution in DAKO antibody diluent; and secondary detection was with DAKO Envision antirabbit horseradish peroxidase polymer. Positive and negative prolactin and growth hormone staining controls were sections of anterior and posterior pituitary, respectively, from normal mouse (see Supplementary Fig. S1).

For quantitation of vascular density, MECA-32-stained sections were analyzed with an Ariol SL-50 slide scanning platform (Applied Imaging) using a 10× objective. Pituitary tumor regions were identified and outlined manually. Pixel colors corresponding to MECA-32 staining were defined and the vascular area was measured accordingly. Tumor cell nuclei were identified by pixel color and object shape. Vascular area was then normalized to pituitary tumor cell number. Pancreatic islets were analyzed similarly, except that MECA-32 staining area was normalized to islet tumor area.

Analysis of serum prolactin and insulin levels. Serum prolactin amount was analyzed by National Hormone & Peptide Program at Harbor University of California at Los Angeles. Serum insulin amount

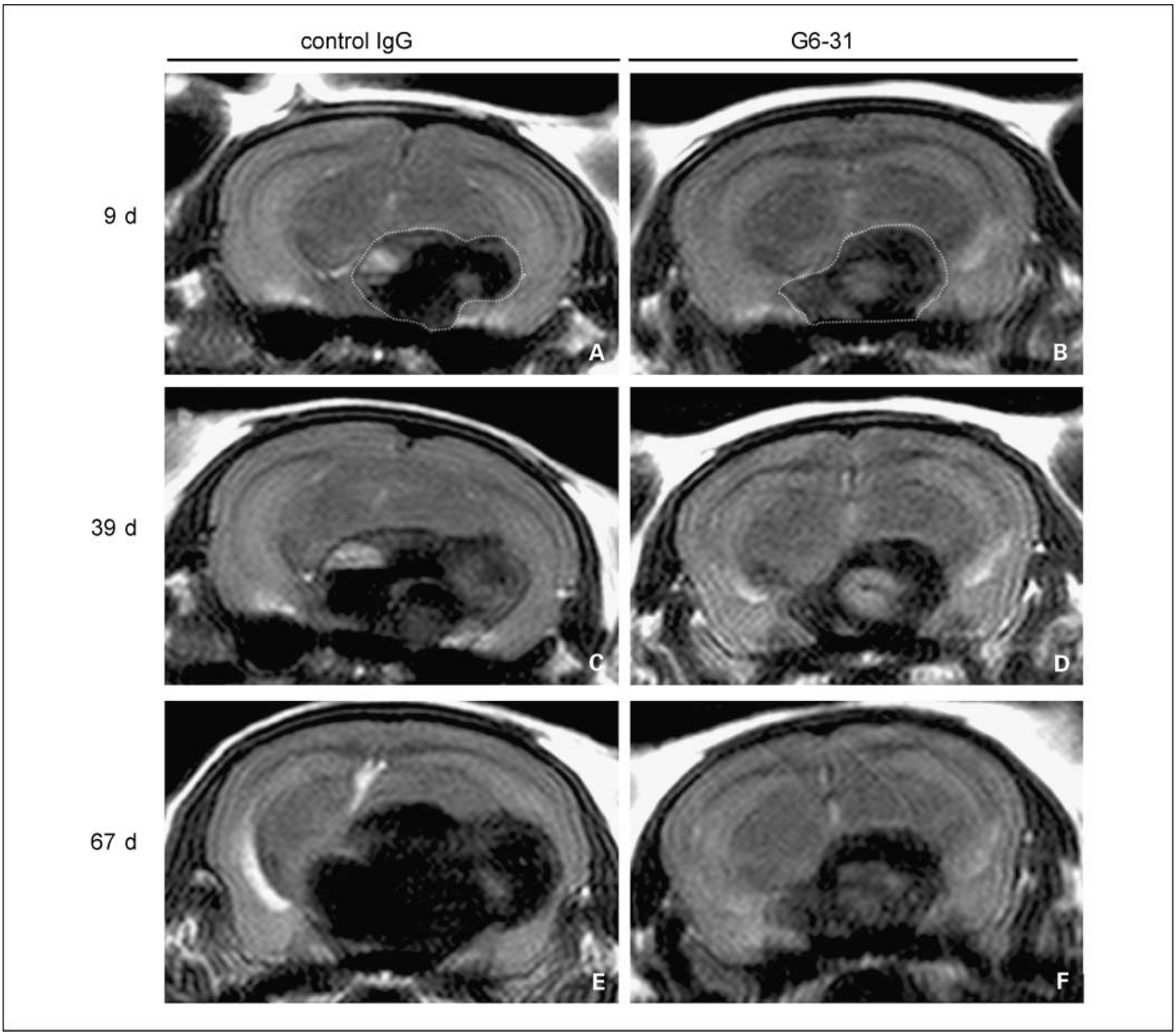

Fig. 2. Magnetic resonance imaging images of representative pituitary tumors from *Men1*$^{+/-}$ mice. A coronal section with a pituitary adenoma from mice treated with control IgG or mAb G6-31 at days 9, 39, and 67 of treatment. For day 9, the edges of the pituitary adenomas have been designated with yellow dotted lines. Volume of the adenoma in the control IgG treated-mouse was 23.2, 55.9, and 142.0 mm^3, and that of the tumor in the mouse treated with mAb G6-31 was 18.9, 27.2, and 35.3 mm^3, at days 9, 39, and 67 of treatment, respectively.

was analyzed using an Ultrasensitive Mouse Insulin ELISA kit according to the manufacturer's instructions (Mercodia).

Results

***Treatment with mAb G6-31 inhibits the growth of* Men1$^{+/-}$ *pituitary adenomas* in situ.** To investigate whether anti–VEGF-A therapy would be effective in inhibiting the growth of pituitary adenomas, 125 eleven- to thirteen-month-old female *Men1*$^{+/-}$ mice were subjected to magnetic resonance imaging to identify mice with pituitary tumors. Tumor-bearing mice were subjected to imaging again 14 and 28 days later to establish the growth rate of the adenomas. A cohort of nine mice with 12.4% mean tumor growth per day and 15.58 ± 4.0 (SE) mm^3 mean tumor volume were assigned to receive control IgG, and a cohort of eight mice with 10.2% mean tumor growth per day and 16.70 ± 5.7 mm^3 mean tumor volume received an anti–VEGF-A mAb G6-31 for 67 days or until mice were found moribund. During the treatment period, animals were imaged with magnetic resonance imaging every 2 weeks to follow up pituitary adenoma growth *in vivo*. At 39 days of treatment, a statistically significant decrease of the mean pituitary tumor volume was observed in the mAb G6-31–treated group compared with the control IgG–treated group (Fig. 1A). At the study end point (67 days), there was a statistically significant 72% (or 3.7-fold) reduction in mean tumor volume on mAb G6-31 treatment ($P < 0.016$). Whereas most (six of nine) control IgG–treated *Men1*$^{+/-}$ tumors continued to grow robustly throughout the treatment period, the growth of seven of eight mAb G6-31–treated pituitary adenomas slowed down

considerably (Fig. 1B). Four mice treated with control IgG and three mice treated with mAb G6-31 were euthanized before the study's end point due to ill health, including one control IgG – treated mouse, before imaging at treatment day 25.

Tumor doubling-free survival was significantly increased in the mAb G6-31 – treated group (log-rank $P < 0.019$; Fig. 1C), suggesting that the inhibition of pituitary tumor growth resulted in health improvement compared with the mice treated with control IgG. The tumor volume of two mice in mAb G6-31 treatment group had not doubled by day 67 of treatment. Graphs of a coronal section of the brain with a representative adenoma from one control IgG – treated and one mAb G6-31 – treated *Men1* $^{+/-}$ mouse are shown in Fig. 2, taken 9, 39, and 67 days after treatment onset.

Anti – VEGF-A antibody inhibits the growth of s.c. pituitary adenoma transplants. To test the efficacy of anti – VEGF-A antibody treatment on a *Men1* $^{+/-}$ pituitary adenoma transplant model, s.c. tumors were established in the flank of BALB/c nude mice. A cohort of 35 mice with a 515 ± 42 mm^3 mean tumor volume at treatment onset received mAb G6-31, and a cohort of 23 mice with a 527 ± 64 mm^3 mean tumor volume at treatment onset received control IgG for 35 days. At treatment end point, tumors from mice treated with control IgG had nearly quadrupled their volumes (mean of 2,071 ± 152 mm^3) whereas tumor growth in mice treated with mAb G6-31 had essentially stopped; the mean tumor volume was 556 ± 89 mm^3 at day 35 (Fig. 1D). There was a statistically significant 73% (or 3.7-fold) reduction in mean tumor volume on mAb G6-31 treatment ($P < 0.0001$).

These data establish that anti – VEGF-A mAb G6-31 is effective in inhibiting the growth of both primary pituitary adenomas and s.c. pituitary adenoma transplants predisposed by heterozygosity of *Men1*.

Expression of VEGF-A, VEGFR-1, VEGFR-2, CD31, and Tie-2 in pituitary tumor tissue. To investigate whether the expression levels of VEGF-A, VEGFR-1, VEGFR-2, CD31, and Tie-2 were affected by mAb G6-31, we measured the mean relative expression of *VEGF-A*, *VEGFR-1*, *VEGFR-2*, *CD31*, and *Tie-2* by quantitative reverse transcription-PCR in five *in situ* pituitary adenomas from mice treated with control IgG (mean volume, 96.2 ± 8.7 mm^3) and five *in situ* pituitary adenomas from mice treated with mAb G6-31 (35.2 ± 4.0 mm^3).

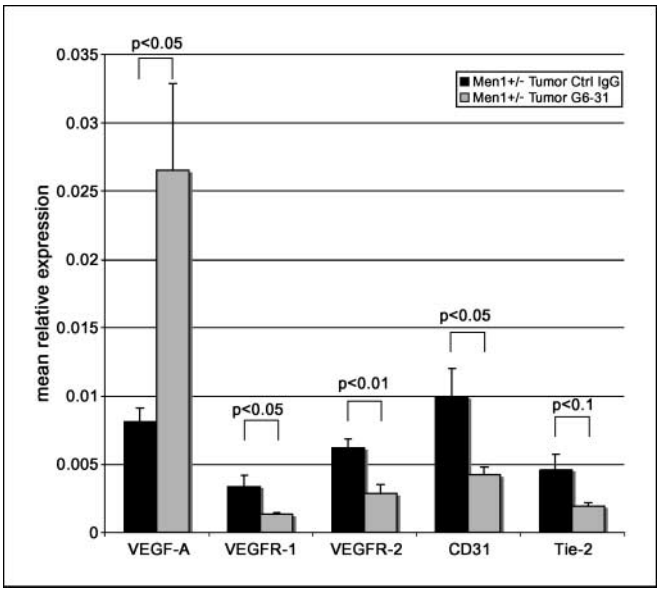

Fig. 3. *Men1* $^{+/-}$ pituitary adenomas express VEGF-A, VEGFR-1, VEGFR-2, CD31, and Tie-2. Columns, mean relative expression of *VEGF-A, VEGFR-1, VEGFR-2, CD31*, and *Tie-2* (compared with endogenous control *GAPDH*) in the pituitary tumors from control IgG – treated *Men1* $^{+/-}$ mice (*black*) and mAb G6-31 – treated *Men1* $^{+/-}$ mice (*gray*); bars, SE.

Notably, the mean relative expression of *VEGF-A* was significantly elevated in *in situ* adenomas from mice treated with mAb G6-31 compared with those from mice treated with control IgG (Fig. 3). In contrast, the mean expression levels of *VEGFR-1*, *VEGFR-2*, *CD31*, and *Tie-2* were significantly lower in the *in situ* tumor samples from mice treated with mAb G6-31 compared with those found in mice treated with control IgG (Fig. 3).

Histology of pituitary and pancreatic tumors. *Men1* $^{+/-}$ pituitary gland adenomas appeared histologically similar in untreated (eight animals examined histologically), mAb G6-31 – treated, and control IgG – treated mice (six animals in each group examined histologically; representative images in Fig. 4A and B). Typically, tumor cells were small (~10 μm in diameter), with a high nuclear/cytoplasmic ratio, often mitotically active, with up to 40 mitotic figures per ten 625-μm-diameter fields. Tumors were variably solid or cystic, with multiple endothelial cell – lined vessels, acutely hemorrhagic areas (intact RBC in non – endothelial-lined spaces, with absence of fibrin or cellular organization), and scattered hemosiderin-laden macrophages, consistent with previous hemorrhage. Tumor vessels were irregularly spaced, typically 5 to 10 μm in diameter although rarely, as large as 50 μm, with few apparent nontumor perivascular stromal cells (Fig. 4C and D). Vessel density was significantly reduced by mAb G6-31 treatment to 46% that of control IgG – treated tumors ($P = 0.009$; Fig. 4E). Notably, in both treatment groups, tumor vascularity was less than in normal adjacent anterior pituitary (data not shown). Pituitary tumors were immunostained for VEGF in both control IgG – and anti-VEGF – treated animals. In control animals, no detectable VEGF was present in tumor cells (Fig. 5A), but rare finely granular signal was localized to tumor endothelium, presumably representing clustered and/or internalized receptor-ligand complexes (Fig. 5C). In tumors treated with anti – VEGF, there were focal areas of VEGF immunostaining in tumor cells (Fig. 5B), which were associated with increased endothelial and stromal VEGF signals (Fig. 5D). The latter may represent VEGF ligand/antibody or ligand/receptor complexes internalized by macrophages, VEGF expression by stromal cells, or both.

Pancreatic islet tumors (reviewed in ref. 31), usually multiple, were invariably identified in 15- to 16-month-old *Men1* $^{+/-}$ mice. Endocrine neoplasms (defined here as being >10^5 μm^2 in the plane of section) were up to 3 mm in diameter in the plane of section, typically solid, occasionally cribriform, generally with minimal mitotic activity, although rare neoplasms had up to 7 mitoses per single high-power field, associated with increased nuclear polymorphism (representative images in Supplementary Fig. S2). Some neoplasms showed stromal hemosiderin-laden macrophages, but there was generally minimal hemorrhage and necrosis (Supplementary Fig. S3). Tumors from six animals treated with anti – VEGF-A mAb G6-31 ($n = 32$ tumors) averaged only 39% the area of those from the five animals treated with control IgG ($n = 45$ tumors;

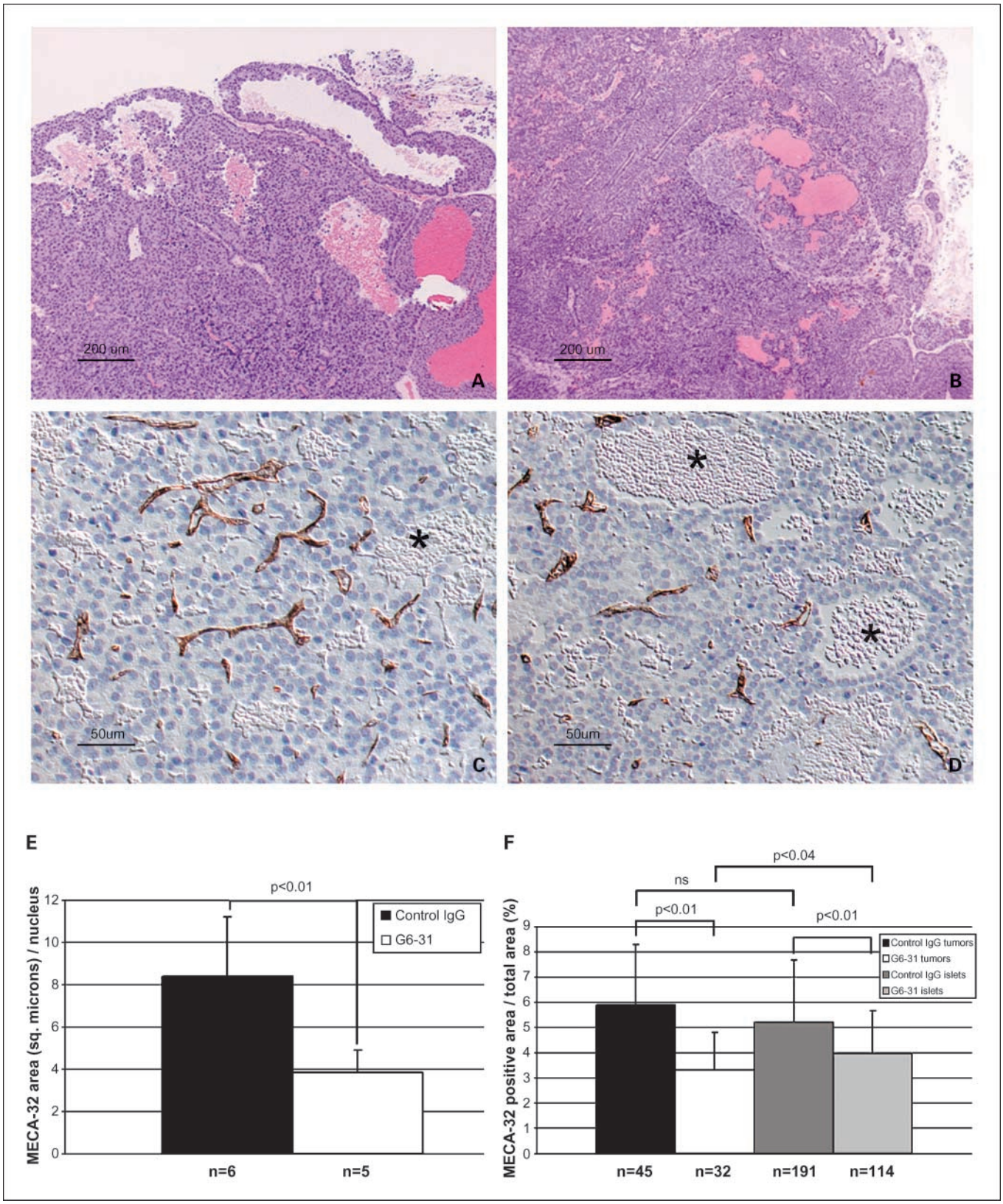

Fig. 4. Vessel density in primary pituitary and pancreatic neuroendocrine tumors of *Men1* $^{+/-}$ mice. Histologic examination of primary pituitary tumors of *Men1* $^{+/-}$ mice. Representative images of pituitary tumor sections stained with H&E (*A* and *B*) or the endothelial marker MECA-32 (*C* and *D*); animals were treated with control IgG (*A* and *C*) or anti-VEGF (*B* and *D*). Cystic blood-filled spaces not lined by endothelial cells (*C* and *D, asterisks*) are typical in the pituitary adenomas. *E,* quantitation of pituitary tumor vascular density (from MECA-32 – stained sections) in control IgG – and anti – VEGF-A – treated animals; bars, SD. *F,* quantitation of vascular density (from MECA-32 – stained sections) in both neuroendocrine tumors and normal pancreatic islets from control IgG – and anti – VEGF-A – treated animals; bars, SD. ns, not significant.

P = 0.026). Vascular density in neuroendocrine tumors was significantly reduced by G6-31 treatment to 56% that of control IgG–treated tumors ($P < 0.0001$; Fig. 4F and Supplementary Fig. S3C and D). In addition, "normal" islets ($<10^5$ μm^2 in the plane of section) from mAb G6-31–treated mice had a vascular density reduced, by a smaller magnitude, to 76% that of control IgG–treated animals ($P < 0.0001$; Fig. 4F). Pancreatic neuroendocrine tumors in control IgG– and anti-VEGF–treated animals were immunostained for VEGF protein (Supplementary Fig. S4). Moderate VEGF signal was present in essentially all cells in normal islets and in islets expanded by neuroendocrine tumors; a minority of tumors had notably stronger VEGF signal than normal islets. Animals treated with anti-VEGF showed no apparent changes in tumor cell VEGF signal, although they did show increased stromal and endothelial VEGF signals, as was noted for pituitary tumors in the same treatment group. A single male animal, treated with control IgG, had a solitary 12-mm-diameter adrenal cortical tumor, a recognized tumor type in the MEN1 syndrome glands (13). Thyroid and parathyroid glands were not examined microscopically.

Histology of the s.c. pituitary adenoma transplants (see Supplementary Fig. S5) was comparable to that of the pituitary tumors *in situ*, indicating a successful recapitulation of endocrine tumor growth at distant loci.

MEN1 pituitary adenomas are prolactinomas. Approximately 60% of pituitary adenomas in MEN1 patients secrete prolactin (PRL), fewer than 25% growth hormone and 5% adrenocorticotropic hormone (14). To investigate whether the pituitary adenomas of *Men1*$^{+/-}$ mice secrete PRL, immunohistochemical staining with anti-PRL antibodies was done on *in situ* pituitary adenomas as well as pituitary tumor transplants from mice treated with control IgG or mAb G6-31. Six of six adenomas from control IgG and five of five from mice treated with mAb

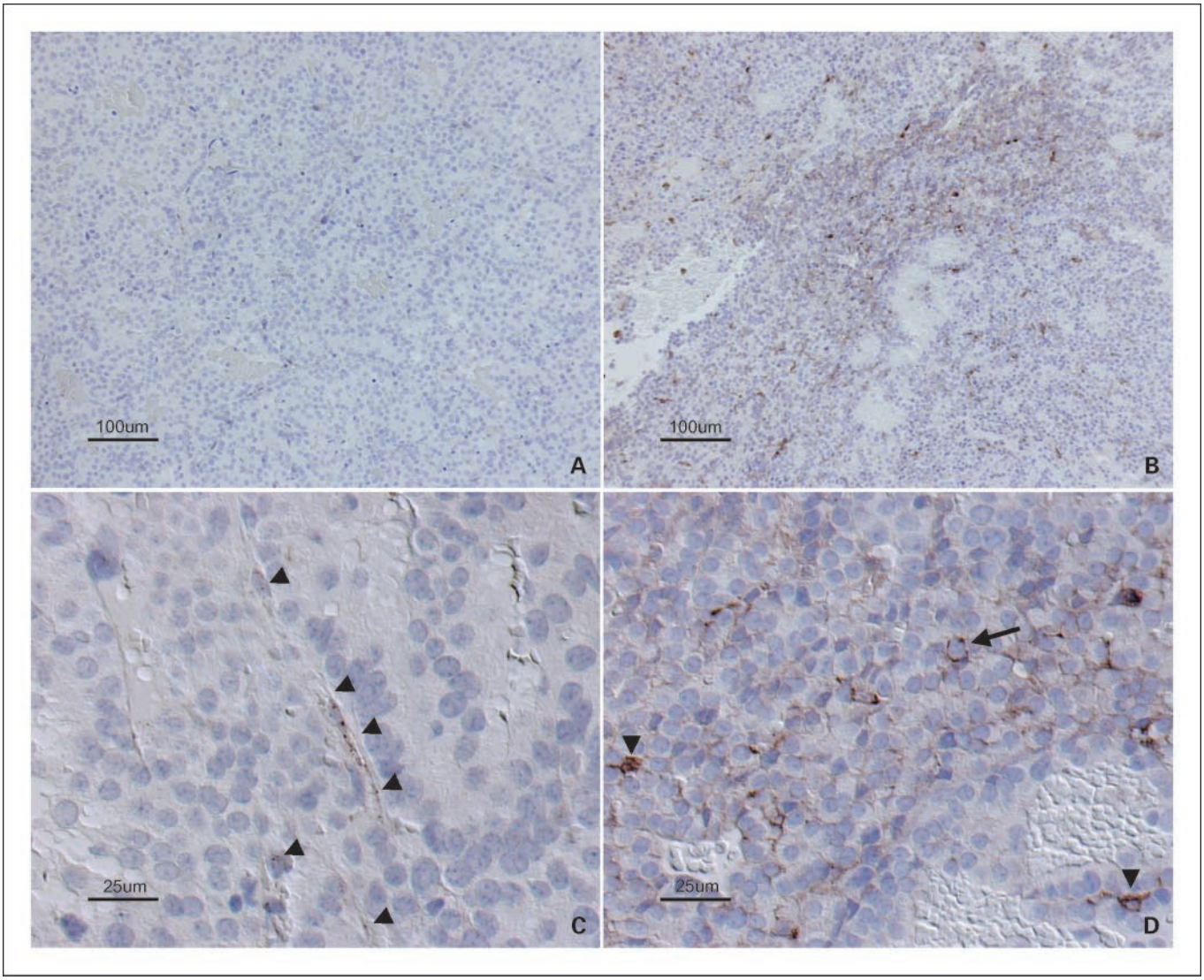

Fig. 5. VEGF immunohistochemistry in pituitary tumors of *Men1*$^{+/-}$ mice. Immunohistochemical detection of VEGF in primary pituitary tumors from animals treated with control IgG (*A* and *C*) and anti-VEGF (*B* and *D*). In control animals, no detectable VEGF signal is present in tumor cells (*A*), but rare granular signal is present in endothelial cells (*C, arrowheads*). Focal weak VEGF signal is present in tumor cells from animals treated with anti-VEGF (*B* and *arrow* in *D*). In addition, animals treated with anti-VEGF showed increased stromal VEGF signal (*D, arrowheads*).

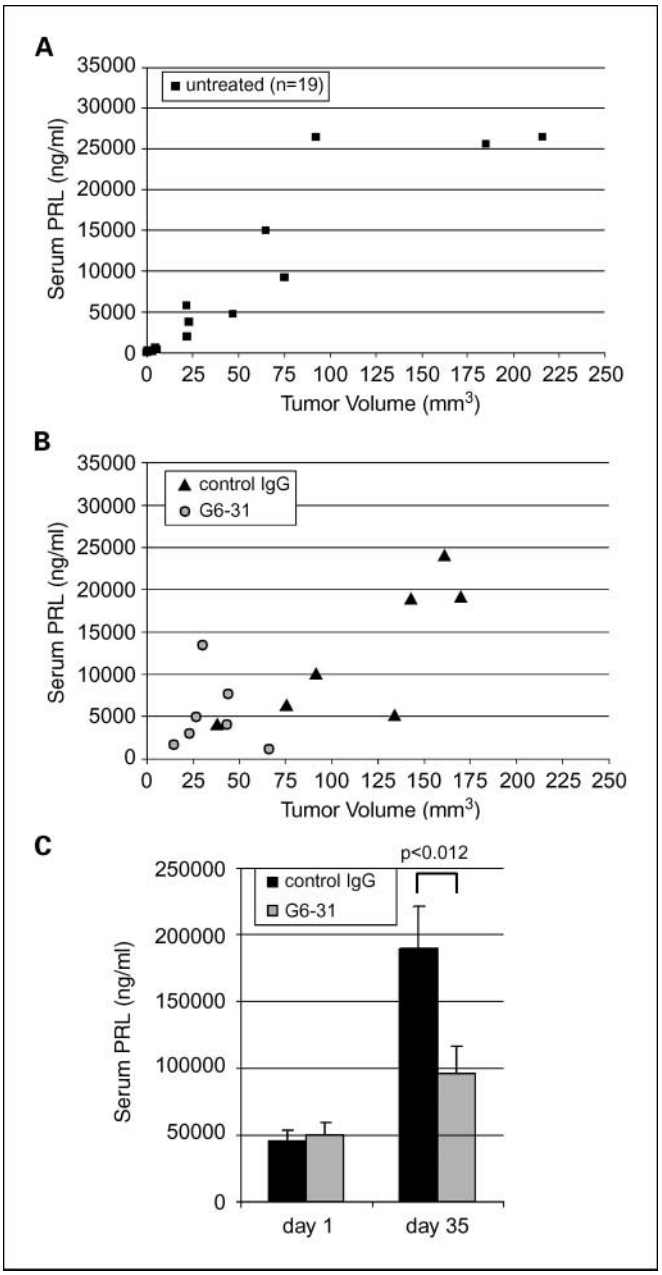

Fig. 6. Serum prolactin level is elevated in mice with pituitary tumors and pituitary tumor transplants. *A,* serum PRL (ng/mL) level plotted against pituitary tumor volume from 19 nontreated tumor-bearing *Men1*$^{+/-}$ mice illustrates positive correlation. *B,* serum PRL level plotted against pituitary tumor volume from *Men1*$^{+/-}$ mice treated with control IgG (*black triangles*) or mAb G6-31 (*gray spheres*) at study end point. *C,* serum PRL from mice with pituitary adenoma transplants at days 1 and 35 of treatment.

G6-31 showed a specific, positive staining for prolactin in ~50% to 95% of the cells, establishing them as prolactinomas (Supplementary Fig. S6A and B). In line with this result, Crabtree et al. (23) reported that *Men1*$^{TSM/+}$ pituitary tumors were positive for PRL in an immunohistochemical staining. Prolactin staining was also positive in the pituitary adenoma transplants with either treatment (Supplementary Fig. S5). Consistent with functional prolactin secretion from these tumors, mammary tissue in female mice bearing transplanted pituitary adenomas invariably showed moderate to marked lactational change in both control IgG– and anti–VEGF-A–treated animals (Supplementary Fig. S5A and B).

As assessed by immunohistochemical staining, 6 of 11 nontreated primary pituitary tumors were focally and weakly positive for growth hormone, whereas only one of four transplanted pituitary tumors showed focal weak staining (not shown). Growth hormone expression was present in both G6-31– and control IgG–treated *in situ* pituitary tumors (Supplementary Fig. S6). Normal anterior pituitary showed strong reactivity in ~20% to 30% of cells (Supplementary Fig. S1).

Serum prolactin level correlates with pituitary tumor volume in untreated and control IgG–treated mice and is decreased by mAb G6-31 treatment. Given that all pituitary adenomas examined from *Men1*$^{+/-}$ mice treated with control IgG or mAb G6-31 were positive for prolactin by immunohistochemical analysis, we investigated whether serum PRL levels were elevated in *Men1*$^{+/-}$ pituitary adenoma–bearing mice. To this end, we initially analyzed 46 nontreated female *Men1*$^{+/-}$ mice for their pituitary tumor status and serum PRL level and five female wild-type littermate controls for serum PRL level. The age range of these mice was 10.5 to 15.6 months, with an average age of 13.3 months.

The mean serum PRL level in the wild-type mice was 44 ± 25 (SE) ng/mL. Twenty-seven of the 46 *Men1*$^{+/-}$ mice did not have a detectable pituitary tumor in magnetic resonance imaging analysis. The mean serum PRL level in these mice was 69 ± 24 ng/mL. Ten mice had a small pituitary tumor with a mean volume of 1.7 ± 0.6 mm^3. Serum PRL level in these mice was elevated to a mean of 188 ± 61 ng/mL. Nine mice that had a large pituitary tumor (mean volume, 83 ± 23 mm^3) had a mean serum PRL of 13,239 ± 3,466 ng/mL. These data establish that there is a positive correlation between serum PRL levels and pituitary tumor volume in the *Men1*$^{+/-}$ mice (Fig. 6A) with Pearson's correlation coefficient $r = 0.94$, suggesting that serum PRL level could be useful as a diagnostic tool in establishing an estimate of pituitary tumor status.

To examine whether anti–VEGF-A treatment had an effect on serum PRL level, we analyzed the serum of seven control IgG– and seven mAb G6-31–treated *Men1*$^{+/-}$ mice with a pituitary adenoma *in situ* at study end point (day 67). In mice treated with control IgG, the mean serum PRL level was elevated to 12,566 ± 3,047 ng/mL and was generally increased with increasing tumor volume (mean of 116.2 ± 18.5 mm^3; $r = 0.80$, $P < 0.03$). In mAb G6-31–treated *Men1*$^{+/-}$ mice analyzed, the serum PRL level remained lower, at 5,163.7 ± 1,608.9 ng/mL. However, no obvious correlation to tumor volume was apparent (mean tumor volume, 35.3 ± 6.5 mm^3; $r = -0.12$ with $P < 0.80$; Fig. 6B). Nonetheless, these data indicate that whereas mAb G6-31 inhibits the pituitary adenoma growth, it also leads to a decreased mean serum PRL compared with control IgG–treated mice ($P < 0.05$).

Treatment with anti–VEGF-A lowers serum PRL in mice with s.c. pituitary tumor transplants. Whereas the above data indicate that anti–VEGF-A antibody treatment lowers the serum level of PRL in tumor-bearing *Men1*$^{+/-}$ mice, we further investigated serum PRL level in the context of the s.c. pituitary adenoma transplants in BALB/c nude mice. Serum PRL was measured from samples originating from 23 control IgG– and 35 mAb G6-31–treated mice, harvested at treatment onset (day 1) and at study end point (day 35). Whereas the mean

serum PRL at day 1 was comparable between the two treatments, at day 35, mAb G6-31 treatment had significantly reduced the serum PRL (Fig. 6C).

Because the current treatment of MEN1 prolactinomas includes medical therapy or selective hypophysectomy followed by radiotherapy, our data indicating that mAb G6-31 treatment leads to lower PRL serum level with a prominent inhibition of tumor growth provide a potential new therapeutic approach to MEN1 patients.

Serum insulin levels are elevated in* Men1$^{+/-}$ *mice. To examine whether the serum insulin levels were elevated in the *Men1*$^{+/-}$ mice, serum samples were analyzed from six nonfasted mice treated with control IgG and six nonfasted mice treated with mAb G6-31, all identified with pancreatic lesions in histologic analysis. Serum insulin levels were also analyzed from five nonfasted, age-matched wild-type mice. No correlation with treatment was observed. However, we observed a trend of elevated mean serum insulin in *Men1*$^{+/-}$ mice (control IgG, 3.8 ± 2.6 ng/mL; mAb G6-31, 3.7 ± 2.4 ng/mL) compared with wild-type mice [1.4 ± 0.7 (SE) ng/mL; $P = 0.13$ and $P = 0.16$, respectively], in agreement with previous data.

Discussion

VEGF-A is necessary for the development of vascularization of pancreatic islets and for the angiogenic switching and carcinogenesis of insulinomas in the RIP-Tag model of islet carcinoma (32). Our data indicate that VEGF-A is also required for the growth of benign pituitary gland adenomas in the mouse model of MEN1 because a monotherapy with a monoclonal antibody targeting VEGF-A was shown to result in substantial tumor growth inhibition. Additionally, we have been able to establish a transplantable model of MEN-1 pituitary tumor, which produces high levels of prolactin and is fully responsive to anti–VEGF-A therapy. Considering the incomplete penetrance and the length of time required for the establishment of the phenotype in mice, the availability of a transplantable model might significantly facilitate the investigation of the mechanisms of MEN1 tumorigenesis and regulation of hormone secretion.

It is conceivable that much of the observed antitumor effects of mAb G6-31 are mediated by suppression of VEGFR-2–dependent angiogenesis. In addition to the observation that the mean expression of VEGFR-2 mRNA in large pituitary adenomas was significantly affected by anti–VEGF-A treatment (Fig. 3), immunohistochemical staining for MECA-32 showed highly significant decreases in vascularity (~50% reduction) in both pituitary and pancreatic neuroendocrine tumors treated with mAb G6-31 (Fig. 4). A corresponding reduction in anti–VEGF-A–treated tumor growth was noted in both pituitary and pancreatic tumors. Vascular density in normal pancreatic islets was also significantly decreased by anti–VEGF-A treatment, although the magnitude of the change (25% reduction from control IgG treated) was less than that seen in pancreatic adenomas.

The observed high level of *VEGF-A* transcript in mAb G6-31–treated tumors is potentially a result of a compensatory mechanism to the systemic sequestering of VEGF-A by mAb G6-31. However, it seemed that such elevated VEGF-A was not sufficient to drive the tumor growth.

In addition to showing that a monotherapy with an anti–VEGF-A mAb significantly lowered the pituitary tumor burden of the *Men1*$^{+/-}$ mice by effectively inhibiting adenoma growth, we show that the serum prolactin levels were significantly lowered. Thus, our data suggest the possibility that VEGF-A blockade may represent a nonsurgical treatment for benign tumors of the endocrine system, possibly in combination with dopamine agonists (in the case of prolactin-secreting adenomas; refs. 33, 34) or other pharmacologic agents.

It is tempting to speculate that VEGF-A inhibition will prove particularly effective in the treatment/prevention of benign tumors. Interestingly, previous studies have shown that anti–VEGF-A mAb G6-31 and AZD2171, a small-molecule inhibitor of VEGFR and fibroblast growth factor receptor signaling (35, 36), inhibit growth of polyps in the *Apc*$^{+/min}$ model of familial adenomatous polyposis (29, 37). However, because a systemic VEGF-A blockade can be associated with some significant side effects in some patients, further understanding of the mechanism of such side effects will be helpful to design clinical trials with VEGF-A inhibitors in benign tumors (38).

References

1. Risau W. Mechanisms of angiogenesis. Nature 1997;386:671–4.
2. Red-Horse K, Crawford Y, Shojaei F, Ferrara N. Endothelium-microenvironment interactions in the developing embryo and in the adult. Dev Cell 2007;12:181–94.
3. Folkman J. Angiogenesis in cancer, vascular, rheumatoid and other disease. Nat Med 1995;1:27–31.
4. Ferrara N, Kerbel RS. Angiogenesis as a therapeutic target. Nature 2005;438:967–74.
5. Turner HE, Harris AL, Melmed S, Wass JA. Angiogenesis in endocrine tumors. Endocr Rev 2003;24:600–32.
6. LeCouter J, Kowalski J, Foster J, et al. Identification of an angiogenic mitogen selective for endocrine gland endothelium. Nature 2001;412:877–84.
7. Ferrara N, Frantz G, LeCouter J, et al. Differential expression of the angiogenic factor genes vascular endothelial growth factor (VEGF) and endocrine gland-derived VEGF in normal and polycystic human ovaries. Am J Pathol 2003;162:1881–93.
8. Samson M, Peale FV, Jr., Frantz G, Rioux-Leclercq N, Rajpert-De Meyts E, Ferrara N. Human endocrine gland-derived vascular endothelial growth factor: expression early in development and in Leydig cell tumors suggests roles in normal and pathological testis angiogenesis. J Clin Endocrinol Metab 2004;89:4078–88.
9. Ferrara N, Gerber HP, LeCouter J. The biology of VEGF and its receptors. Nat Med 2003;9:669–76.
10. Roy H, Bhardwaj S, Yla-Herttuala S. Biology of vascular endothelial growth factors. FEBS Lett 2006;580:2879–87.
11. Ferrara N. Vascular endothelial growth factor: basic science and clinical progress. Endocr Rev 2004;25:581–611.
12. Olsson AK, Dimberg A, Kreuger J, Claesson-Welsh L. VEGF receptor signalling—in control of vascular function. Nat Rev Mol Cell Biol 2006;7:359–71.
13. Thakker RV. Multiple endocrine neoplasia type 1. In: Endocrinology. DeGroot LJ, Jameson JL, editors. Elsevier Saunders; 2006. p. 3509–31.
14. Trump D, Farren B, Wooding C, et al. Clinical studies of multiple endocrine neoplasia type 1 (MEN1). QJM 1996;89:653–69.
15. Chandrasekharappa SC, Guru SC, Manickam P, et al. Positional cloning of the gene for multiple endocrine neoplasia-type 1. Science 1997;276:404–7.
16. Pannett AA, Thakker RV. Multiple endocrine neoplasia type 1. Endocr Relat Cancer 1999;6:449–73.
17. Bystrom C, Larsson C, Blomberg C, et al. Localization of the MEN1 gene to a small region within chromosome 11q13 by deletion mapping in tumors. Proc Natl Acad Sci U S A 1990;87:1968–72.
18. Debelenko LV, Zhuang Z, Emmert-Buck MR, et al. Allelic deletions on chromosome 11q13 in multiple endocrine neoplasia type 1-associated and sporadic gastrinomas and pancreatic endocrine tumors. Cancer Res 1997;57:2238–43.
19. Larsson C, Skogseid B, Oberg K, Nakamura Y, Nordenskjold M. Multiple endocrine neoplasia type 1 gene maps to chromosome 11 and is lost in insulinoma. Nature 1988;332:85–7.

20. Agarwal SK, Kennedy PA, Scacheri PC, et al. Menin molecular interactions: insights into normal functions and tumorigenesis. Horm Metab Res 2005;37:369–74.

21. Brandi ML, Gagel RF, Angeli A, et al. Guidelines for diagnosis and therapy of MEN type 1 and type 2. J Clin Endocrinol Metab 2001;86:5658–71.

22. Viola KV, Sosa JA. Current advances in the diagnosis and treatment of pancreatic endocrine tumors. Curr Opin Oncol 2005;17:24–7.

23. Crabtree JS, Scacheri PC, Ward JM, et al. A mouse model of multiple endocrine neoplasia, type 1, develops multiple endocrine tumors. Proc Natl Acad Sci U S A 2001;98:1118–23.

24. Kim KJ, Li B, Winer J, et al. Inhibition of vascular endothelial growth factor-induced angiogenesis suppresses tumor growth *in vivo*. Nature 1993;362:841–4.

25. Gerber HP, Kowalski J, Sherman D, Eberhard DA, Ferrara N. Complete inhibition of rhabdomyosarcoma xenograft growth and neovascularization requires blockade of both tumor and host vascular endothelial growth factor. Cancer Res 2000;60:6253–8.

26. Holash J, Davis S, Papadopoulos N, et al. VEGF-Trap: a VEGF blocker with potent antitumor effects. Proc Natl Acad Sci U S A 2002;99:11393–8.

27. Prewett M, Huber J, Li Y, et al. Antivascular endothelial growth factor receptor (fetal liver kinase 1) monoclonal antibody inhibits tumor angiogenesis. Cancer Res 1999;59:5209–18.

28. Manley PW, Martiny-Baron G, Schlaeppi JM, Wood JM. Therapies directed at vascular endothelial growth factor. Expert Opin Investig Drugs 2002;11:1715–36.

29. Korsisaari N, Kasman IM, Forrest WF, et al. Inhibition of VEGF-A prevents the angiogenic switch and results in increased survival of $Apc^{+/min}$ mice. Proc Natl Acad Sci U S A 2007;104:10625–30.

30. Liang WC, Wu X, Peale FV, et al. Cross-species vegf-blocking antibodies completely inhibit the growth of human tumor xenografts and measure the contribution of stromal vegf. J Biol Chem 2006;281:951–61.

31. Frankel WL. Update on pancreatic endocrine tumors. Arch Pathol Lab Med 2006;130:963–6.

32. Inoue M, Hager JH, Ferrara N, Gerber HP, Hanahan D. VEGF-A has a critical, non redundant role in angiogenic switching and pancreatic β cell carcinogenesis. Cancer Cell 2002;1:193–202.

33. Melmed S. Mechanisms for pituitary tumorigenesis: the plastic pituitary. J Clin Invest 2003;112:1603–18.

34. Gillam MP, Molitch ME, Lombardi G, Colao A. Advances in the treatment of prolactinomas. Endocr Rev 2006;27:485–94.

35. Wedge SR, Kendrew J, Hennequin LF, et al. AZD2171: a highly potent, orally bioavailable, vascular endothelial growth factor receptor-2 tyrosine kinase inhibitor for the treatment of cancer. Cancer Res 2005;65:4389–400.

36. Takeda M, Arao T, Yokote H, et al. AZD2171 shows potent antitumor activity against gastric cancer overexpressing fibroblast growth factor receptor 2/keratinocyte growth factor receptor. Clin Cancer Res 2007;13:3051–7.

37. Goodlad RA, Ryan AJ, Wedge SR, et al. Inhibiting vascular endothelial growth factor receptor-2 signaling reduces tumor burden in the $Apc^{Min/+}$ mouse model of early intestinal cancer. Carcinogenesis 2006;27:2133–9.

38. Ferrara N, Mass RD, Campa C, Kim R. Targeting VEGF-A to treat cancer and age-related macular degeneration. Annu Rev Med 2007;58:491–4.

Clinical Cancer Research

Blocking Vascular Endothelial Growth Factor-A Inhibits the Growth of Pituitary Adenomas and Lowers Serum Prolactin Level in a Mouse Model of Multiple Endocrine Neoplasia Type 1

Nina Korsisaari, Jed Ross, Xiumin Wu, et al.

Clin Cancer Res 2008;14:249-258.